Towards an enhanced performance of uniform circular arrays at low frequencies

Tiana Roig, Elisabet; Torras Rosell, Antoni; Fernandez Grande, Efren; Jeong, Cheol-Ho; Agerkvist, Finn T.

Published in:
Proceedings of INTER-NOISE 2013

Publication date:
2013

Towards an enhanced performance of uniform circular arrays at low frequencies

Elisabet Tiana-Roig [1], Antoni Torras-Rosell [2], Efren Fernandez-Grande [3], Cheol-Ho Jeong [4], and Finn T. Agerkvist [5]

[1, 3, 4, 5]Acoustic Technology, Dep. Electrical Engineering,

Technical University of Denmark, Ørsteds Plads 352, 2800 Kgs. Lyngby, Denmark

[2]DFM, Danish National Metrology Institute,

Matematiktorvet 307, 2800 Kgs. Lyngby, Denmark

ABSTRACT

Beamforming using uniform circular arrays of microphones can be used, e.g., for localization of environmental noise sources and for conferencing. The performance depends strongly on the characteristics of the array, for instance the number of transducers, the radius and whether the microphones are mounted on a scatterer such as a rigid cylinder or a sphere. The beamforming output improves with increasing frequency, up to a certain frequency where spatial aliasing occurs. At low frequencies the performance is limited by the radius of the array; in other words, given a certain number of microphones, an array with a larger radius will perform better than a smaller array. The aim of this study is to improve the performance of the array at low frequencies without modifying its physical characteristics. This is done by predicting the sound pressure at a virtual and larger concentric array. The propagation of the acoustic information captured by the microphones to the virtual array is based on acoustic holography. The predicted pressure is then used as input of the beamforming procedure. The combination of holography and beamforming for enhancing the beamforming output at low frequencies is examined with computer simulations and experimental results.
Keywords: Uniform circular array, Beamforming, Holography

1. INTRODUCTION

Beamforming based on a uniform circular array of microphones (UCA) is a well-known method to localize sound sources around the array from 0 to 360°. In the present paper, the main concern is the improvement of the performance at low frequencies. In the recent years, various strategies have been suggested

[1] etr@elektro.dtu.dk
[2] atr@dfm.dk
[3] efr@elektro.dtu.dk
[4] chj@elektro.dtu.dk
[5] fa@elektro.dtu.dk

in this matter, such as the design of beamforming techniques other than delay-and-sum. For instance, circular harmonics beamforming is a clear example of how a beamforming technique can be designed to suit a particular geometry, in this case, the circular geometry. This technique is based on the decomposition of the sound field in a series of coefficients by means of a Fourier series.[1] With this technique most of the frequency range is improved. Another possibility is to flush-mount the microphones on a rigid baffle, such as a rigid sphere or a spherical cylinder. The effect of the scatterer has proved to be beneficial compared to the case where the array microphones are suspended in the free space.[2–4] Yet another alternative is the use of deconvolution methods, which clean the beamforming map by means of iterative algorithms to finally recover the distribution of the sources present in the sound field. These methods are very effective, but require high computational effort, in particular at low frequencies. Methods such as the Deconvolution Approach for the Mapping of Acoustic Sources 2 (DAMAS2), the Fourier-based Non-Negative Least Squares (FFT-NNLS) and the Richardson-Lucy (RL) have already been adapted to the circular geometry.[5,6]

In all cases the performance improves with increasing frequency, up to a frequency where spatial aliasing occurs. The poor performance at the lowest frequencies is especially of concern with delay-and-sum because this presents an omnidirectional pattern, and therefore sources in this frequency range cannot be localized. Although the use of a scatterer improves its performance, it does not completely eliminate this problem. With deconvolution methods the low frequency problems can be resolved, even with beamforming patterns obtained originally with delay-and-sum. However if the same resolution is to be achieved in the entire frequency range, the lower the frequency the more the iterations needed. Or in other words, the deconvolution methods are less efficient at low frequencies.

In this article we suggest a simple method to improve the performance of UCAs at low frequencies, which does not imply the design of new beamforming techniques or a modification of the geometry of the array. The basic idea is that for a specific number of microphones, a UCA with a larger radius will perform better at low frequencies than an array with a smaller radius, because the distance between the microphones will be larger, and the wavelengths corresponding to the low frequencies will be better captured. Inspired by this concept, one could measure the sound field with a UCA, and by means of acoustic holography predict the sound pressure at a larger and virtual radius. The estimated pressure could be then used as input to the beamforming algorithm. A sketch of the procedure can be seen in Fig. 1.

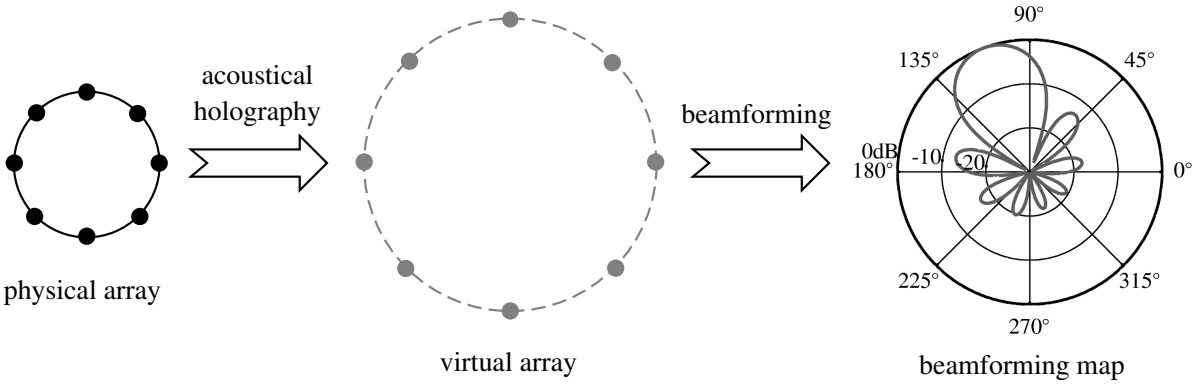

Fig. 1 – Sketch of the procedure for the calculation of the beamforming map. The pressure captured by a UCA is used for the prediction of the pressure at a larger and virtual array by means of acoustical holography. The predicted pressure is used as input of the beamforming procedure.

The combination of holography and beamforming for the improvement of the performance at low frequencies is the subject of study in the present work, and this is examined by means of computer simulations and experiments.

2. BACKGROUND THEORY

2.1. Acoustic Holography

Acoustic holography is a sound visualization technique that makes it possible to reconstruct the sound field over a three-dimensional space based on a two dimensional measurement. Often, the measurement is performed close to the source, as in near-field acoustic holography (NAH) to capture the evanescent waves for an enhanced spatial resolution.[7,8] However, in the present study we are concerned with the reconstruction of the sound field in the far field, prior to the beamforming processing.

In acoustic holography, the measured sound field is typically expanded into a series of basis functions from which the entire acoustic field can be reconstructed. In this paper we focus on a circular space, making use of the fact that the sound field can be predicted on different radii by means of the Bessel functions that account for the propagation in the radial direction. This approach is in a sense analogous to the one commonly used for NAH in spherical coordinates,[9–11] but in this case the radial functions are conventional Bessel functions, and the angular dependency is reduced to the azimuth only, as it follows from a circular harmonic expansion. It is worth noting that the inverse holographic reconstruction, i.e., when propagating towards the source, is an ill-posed problem that requires regularization. It has been shown that in the case of spherical NAH, truncation is an appropriate regularization procedure.[12] Similarly, truncation is adequate for the circular geometry.

Let us consider that a plane wave that travels perpendicularly to the z-axis (i.e., the wavefronts are parallel to the z-axis) is captured by a UCA of radius R placed at the xy-plane, at $z = 0$. The sound pressure at the array can be represented in terms of solutions of the Helmholtz equation in a cylindrical coordinate system with origin at the center of the UCA. After applying the boundary conditions (basically that the sound field at the origin must be finite), the pressure can be expressed as[7]

$$p(kr, \varphi) = \sum_{n=-\infty}^{\infty} A_n J_n(kr) e^{jn\varphi}, \tag{1}$$

where k is the wavenumber and A_n is the coefficient of the n'th term. As can be seen the angular dependency of the pressure is given by the circular harmonics $e^{jn\varphi}$, whereas the radial dependency is given by the Bessel functions J_n. Note that the time dependency $e^{-j\omega t}$ is omitted. The previous expression can be ideally used to determine a particular sound field at any point by means of acoustic holography. For this purpose we need to determine the values of the coefficients A_n. The pressure at the UCA, at $r = R$ is

$$p(kR, \varphi) = \sum_{n=-\infty}^{\infty} A_n J_n(kR) e^{jn\varphi}. \tag{2}$$

Making use of the orthogonality of the circular harmonics,

$$\frac{1}{2\pi} \int_0^{2\pi} e^{jn\varphi} e^{-jm\varphi} d\varphi = \delta_{mn}, \tag{3}$$

the coefficients A_n can be retrieved by multiplying each side of Eq. (2) by a complex conjugated circular harmonic and integrating over the entire circle, from 0 to 2π. The resulting expression follows

$$A_n = \frac{\frac{1}{2\pi} \int_0^{2\pi} p(kR, \varphi) e^{-jn\varphi} d\varphi}{J_n(kR)}. \tag{4}$$

This expression implies a continuous integral of the sound pressure. However the pressure is known at discrete positions, because the sound field is sampled with M microphones. Therefore, the integral must be approximated by means of a finite summation:

$$\int_0^{2\pi} p(kR, \varphi) e^{-jn\varphi} d\varphi \quad \Rightarrow \quad \sum_{i=1}^{M} \alpha_i p(kR, \varphi_i) e^{-jn\varphi_i}, \tag{5}$$

where the coefficients α_i must equal $2\pi/M$ to keep the orthogonality properties of the circular harmonics given in Eq. (3) in discrete notation. Finally the coefficients A_n are calculated as

$$\hat{A}_n = \frac{\frac{1}{M} \sum_{i=1}^{M} p(kR, \varphi_i) e^{-jn\varphi_i}}{J_n(kR)}. \tag{6}$$

By inserting this expression into Eq. (1), the sound pressure can be, in principle, predicted anywhere. As mentioned earlier, regularization is needed in practice. This is done by truncating the limits of the summation presented in Eq. (2) to certain values $-N$ and N,

$$p(kr, \varphi) = \sum_{n=-N}^{N} \hat{A}_n J_n(kr) e^{jn\varphi}. \tag{7}$$

It can be shown that a reasonable value of N follows $N = \lceil kr \rceil + 1$, where $\lceil \cdot \rceil$ is the ceiling function, up to a maximum value $M/2 - 1$.

2.2. Beamforming

Beamforming is a signal processing technique commonly used in acoustics to localize sound sources. The beamforming technique used in the present study is the classical delay-and-sum beamforming, which is a very simple, but robust, method. It is based on delaying the signals of each array microphone by a certain amount and adding them together, to reinforce the resulting signal. Depending on the delay applied to the different microphones the array is steered to a particular direction.[13] Expressed in the spatial frequency domain the beamforming output follows

$$b(kR,\varphi) = A\sum_{m=1}^{M} w_i \tilde{p}(kR,\varphi_m)p^*(kR,\varphi_m), \tag{8}$$

where w_m is the weighting coefficient of the m'th microphone, $\tilde{p}(kR,\varphi_m)$ is the pressure measured at the m'th microphone, and $p^*(kR,\varphi_m)$ is the theoretical complex conjugated pressure due to a plane wave with origin at φ. In the presence of a single source, when the beamformer is focused to the direction of the actual source, the maximum output is achieved. Ideally the beamformer would present a peak at the direction of the source and zeros elsewhere, but this is not the case due to the fact that the sound field is captured at discrete positions with the microphones. This implies that the beamforming map presents a main lobe around the direction of the source and side lobes elsewhere.

In case of an unbaffled UCA, the theoretical pressure is simply the closed form for a plane wave, $e^{j\boldsymbol{k}\cdot\boldsymbol{r}}$, at the array microphones, so the beamformer output is

$$b(kR,\varphi) = \frac{1}{M}\sum_{m=1}^{M} \tilde{p}(kR,\varphi_m)e^{jkR\cos(\varphi_m-\varphi)}. \tag{9}$$

Note that the weights w_m have been set to 1 and $A = 1/M$, in order to have a maximum beamformer output equal to one when a plane wave of amplitude unity is present.

Although the focus of the current study is the improvement of the performance at low frequencies, it should be mentioned that the operation of a beamformer is limited at high frequencies when the Nyquist sampling criterion is not fulfilled, i.e., at those frequencies whose corresponding wavelengths are less than twice the distance between two adjacent microphones. When aliasing occurs side lobes increase dramatically, becoming replicas of the main lobe in the worst case (the so-called aliased lobes).

2.3. Combining acoustic holography with beamforming

The aim of this study is to combine acoustic holography and beamforming to improve the beamforming output at low frequencies. As shown in Fig. 1 the pressure is measured with a UCA of radius R and M microphones placed at φ_i. By means of holography the pressure is predicted at a larger and virtual array of radius R_v. In the present study the number of virtual microphones and their azimuth angles are the same as for the actual array. In fact, by means of simulations it has been observed that the position of the microphones is not that relevant as long as the distance between microphones remains constant. This makes sense since UCAs are practically shift-invariant, i.e., the beamforming pattern is the same regardless the focusing direction.[14]

The pressure predicted with acoustic holography, which follows from evaluating Eq. (1) at (R_v,φ_i), is then used as input of the beamforming procedure. The coefficients $\hat{A}_n$ given in Eq. (6) are obtained with the pressure measured with the actual array microphones. Then the beamforming algorithm follows from inserting Eqs. (6) and (7) into Eq. (9),

$$b(kR_v,\varphi) = \frac{1}{M^2}\sum_{m=1}^{M}\sum_{n=-N}^{N}\sum_{i=1}^{M} \tilde{p}(kR,\varphi_i)\frac{J_n(kR_v)}{J_n(kR)}e^{j(n(\varphi_m-\varphi_i)+kR_v\cos(\varphi_m-\varphi))}, \tag{10}$$

where $N = \lceil kR_v \rceil + 1$, up to a maximum value $M/2-1$.

3. RESULTS AND DISCUSSION

3.1. Computer simulations

The effect of combining beamforming and holography is analyzed in this section by means of computer simulations. A UCA like the one shown in Fig. 2 has been assumed. The array radius is $R = 11.9$ cm and it has 12 microphones. The array used for the simulations coincides with the array used for the measurements

Fig. 2 – Prototype UCA of radius 11.9 cm and 12 microphones used for the measurements.

presented in the next section. Following from the Nyquist sampling theorem, this array will present spatial aliasing from ca. 2.8 kHz.

A plane wave generated at $180°$ is considered. The frequency range of interest is from 50 Hz to 2 kHz. A signal-to-noise ratio (SNR) of 30 dB at each array microphone due to uniformly distributed noise is assumed for the simulations to account for background noise.

Beamforming has been performed in the usual way with the pressure at the array microphones following from Sec. 2.2. Besides this, by means of holography, the simulated pressure has been used to predict the pressure at a larger and virtual radius, twice the size of the actual array radius ($2R$) at the same azimuth angles. The predicted pressure at the virtual array has been used for the beamforming procedure as indicated in Sec. 2.3. In parallel, beamforming has been performed in ideal conditions (in absence of noise) with a UCA of radius $2R$ and 12 microphones. Note that for this case, as well as for the case of the virtual array, aliasing is expected from about 1.4 kHz; i.e., the operating frequency range is half the range of the array of radius R.

For ease of understanding the resulting normalized beamforming outputs for a single frequency, in this case 400 Hz, are shown in Fig. 3. It can be seen that in all cases a main lobe around $180°$ is present, which

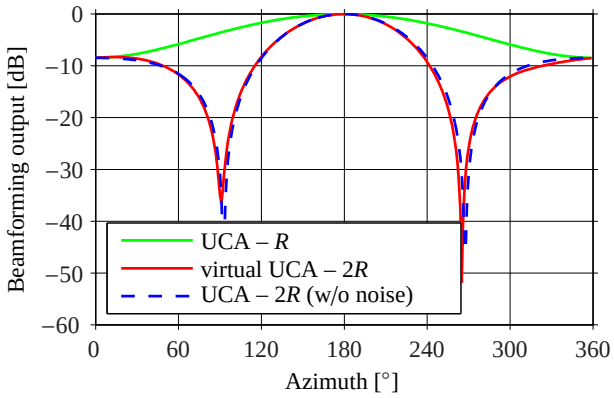

Fig. 3 – Normalized beamforming outputs at 400 Hz obtained with three UCAs with 12 microphones: a real array of radius $R = 11.9$ cm, a virtual array of radius $2R$ and a real array of radius $2R$.

indicates that there is a source in this direction, as expected. However the main lobe obtained with the array with radius R is very wide, which can lead to confusion, whereas the virtual array and the array with radius $2R$ present a narrower main lobe, which makes the interpretation of the map clearer.

The maps obtained for all frequencies are shown in Fig. 4. Note that Fig. 3 corresponds to a vertical cut

of the beamforming maps at 400 Hz.

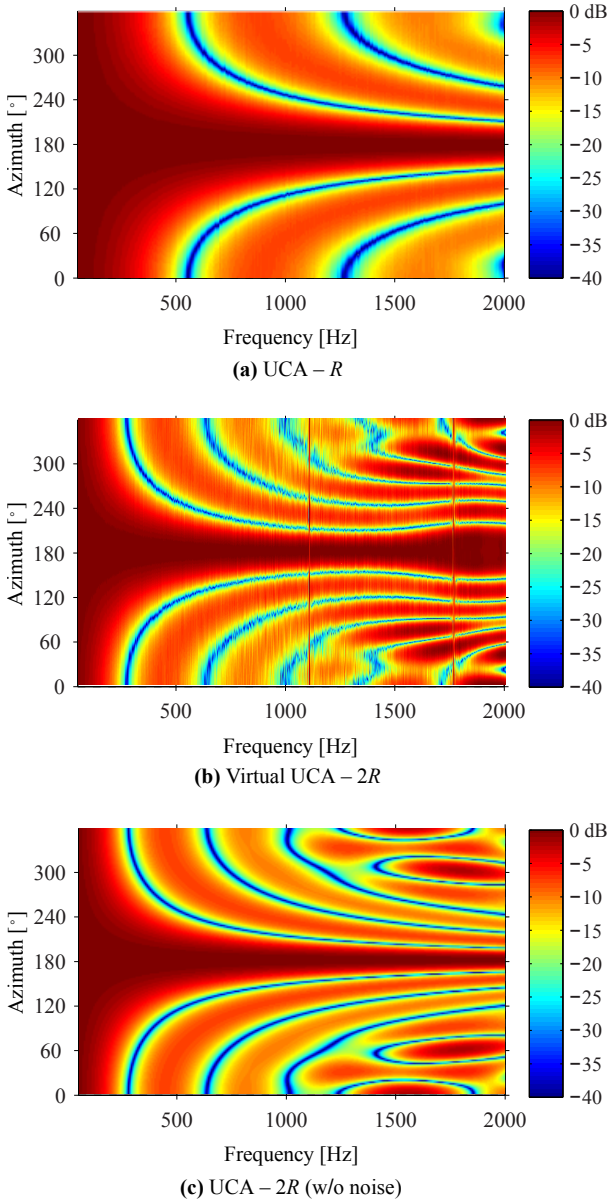

(a) UCA – R

(b) Virtual UCA – $2R$

(c) UCA – $2R$ (w/o noise)

Fig. 4 – Normalized beamforming maps obtained with three UCAs with 12 microphones. (Top) map obtained with an array of radius $R = 11.9$ cm, (middle) map obtained with a virtual array of radius $2R$ by means of combining holography and beamforming, and (bottom) ideal map obtained with an array of radius $2R$. A source at $180°$ is assumed. For the small and the virtual array a SNR of 30 dB is accounted for.

In all the cases the maps are omnidirectional at the lowest frequencies. With increasing frequency the patterns become more directive, unveiling a source at $180°$. For the virtual array and the array of radius $2R$ aliasing is observed at about 1.4 kHz as expected.

The virtual array is more directive at low frequencies compared to the actual array of radius R as expected from the theory. In fact the virtual array is omnidirectional in a narrower frequency range (half the range of the actual array) and from the upper frequency limit of the omnidirectional range it becomes more and more directive. Regarding the level of the side lobes, it can be seen that in both cases the levels are similar.

The performance of the virtual array is very similar to the ideal performance of the array of radius $2R$, up to the Nyquist sampling frequency where differences are observed. This shows that the virtual array behaves in this range as a real array with the same radius. The most apparent difference is the vertical line at 1103 Hz, which shows that for that frequency the beamforming is rather omnidirectional. This is caused by the fact

that the Bessel function in the denominator of Eq. (10) is zero for $n = 0$ at that frequency.

Alternatively to the beamforming maps, the performance of the array can be analyzed by means of two measures: the resolution and the maximum side lobe level (MSL). The resolution is the -3 dB width of the main lobe, whereas the MSL is the difference between the highest secondary lobe and the main lobe. In both cases, the smaller the values, the better. The resolution and the MSL are shown in Fig. 5.

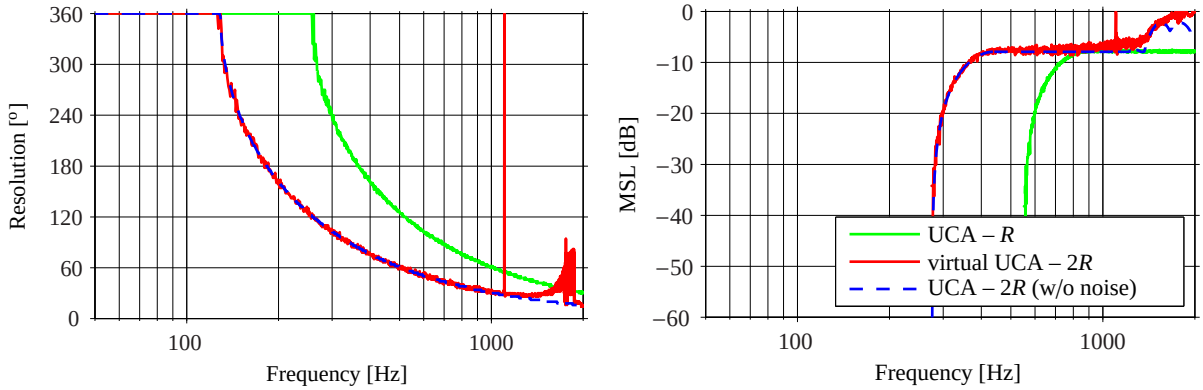

Fig. 5 – Resolution (left) and MSL (right) obtained with UCA of radius $R = 11.9$ cm and 12 microphones, a virtual UCA with radius $2R$, and an ideal UCA of radius $2R$. A plane wave created by a source at $180°$ is assumed. For the small array and the virtual array a SNR of 30 dB is considered.

These two measures confirm that the virtual array behaves like a real array with the same dimensions, especially in terms of resolution, up to the frequencies where sampling error occurs. However, in terms of MSL the levels are slightly higher for the virtual array from about 800 Hz. The peak at 1103 Hz seen in both the resolution and MSL with the virtual array corresponds to the singularity observed previously in the beamforming map.

3.2. Experimental results

Measurements with the prototype array with radius 11.9 cm and 12 microphones shown in Fig. 2 were carried out in an anechoic room of dimensions 12.1 m $\times$ 9.7 m $\times$ 8.5 m. The array microphones were 1/4 in. microphones Brüel & Kjær (B&K) Type 4935.

A picture of the set-up is shown in Fig. 6. The array and the source placed in the far-field of the array were controlled by a B&K PULSE analyzer. The loudspeaker was driven with a signal from the generator, pseudorandom noise of 1 s of period, 3.2 kHz of bandwidth, and 1 Hz of resolution. Each microphone signal was recorded with the analyzer, and after Fourier transforming they were postprocessed with beamforming. The resulting map can be seen in the top panel of Fig. 7.

The data from the microphones were used to predict the pressure by means of acoustical holography at a virtual UCA with twice the radius of the array used for the measurements. With the predicted pressure used as input of the beamforming algorithm, the normalized map shown in the bottom of Fig. 7 was obtained. As can be seen the beamforming maps are very similar to the maps obtained with simulations in the previous section, although they appear slightly more blurry.

The resolution and the MSL for the actual and the virtual arrays can be seen in Fig. 8. These two measures resemble the curves obtained with simulations. In terms of the resolution, the major differences are observed in the peak at 1103 Hz, which is more abrupt, and in the region where aliasing occurs, although this region is not of interest. For the MSL it can be seen that the curves appear slightly shifted towards high frequencies compared with the simulations, and that the MSL of the virtual array is a bit higher than expected in the range between 800 Hz and 1 kHz.

In any case, the results prove that at the low frequencies the actual (and small) array benefits from using holography to predict the pressure at a larger and virtual radius and combine it with beamforming.

4. FINAL REMARKS AND FUTURE WORK

In this article it has been shown that the performance of delay-and-sum beamforming improves at low frequencies by combining acoustic holography with beamforming. The procedure is the following: the pressure captured by a UCA is used to predict the pressure at a virtual array with a larger radius by means of

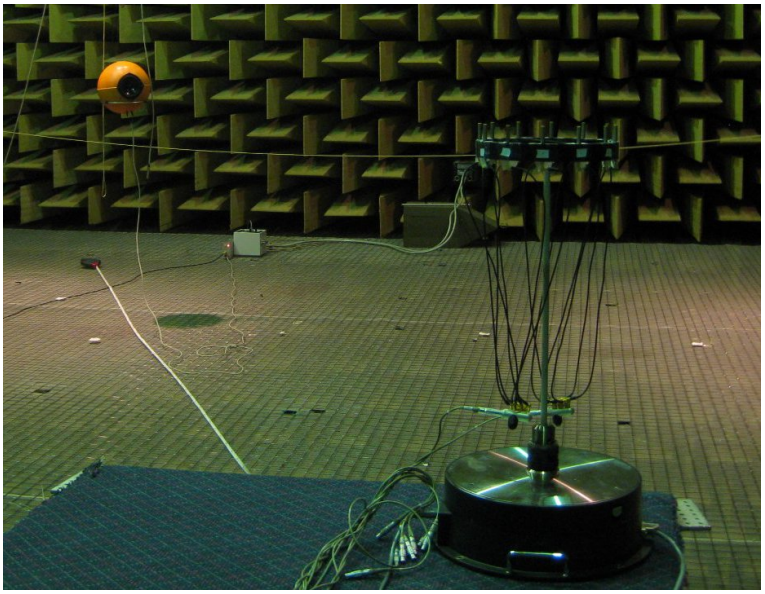

Fig. 6 – Measurement set-up.

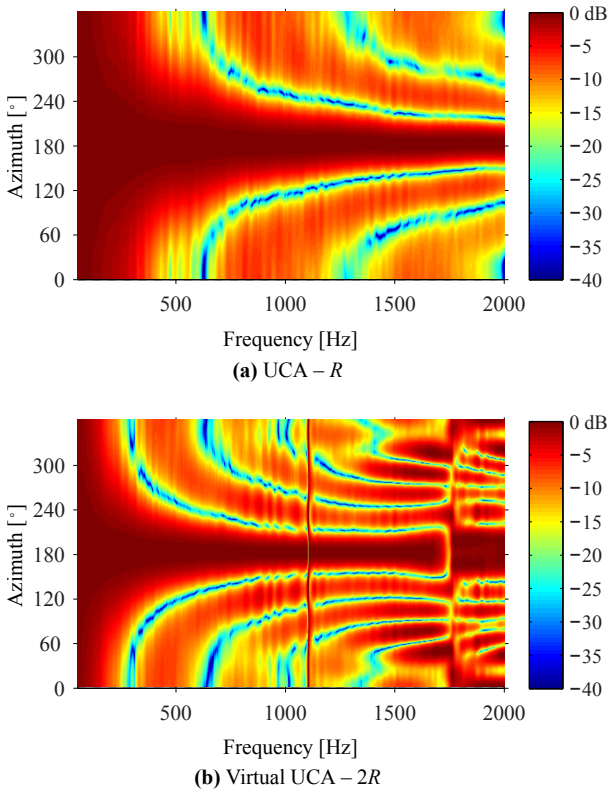

(a) UCA – R

(b) Virtual UCA – $2R$

Fig. 7 – (Top) Normalized beamforming map obtained with a UCA with 12 microphones and radius 11.9 cm. The pressure captured by the array microphones is used to predict the pressure at a virtual UCA with twice the radius of the original array by means of acoustical holography. The predicted pressure is used to compute the normalized beamfroming map (bottom).

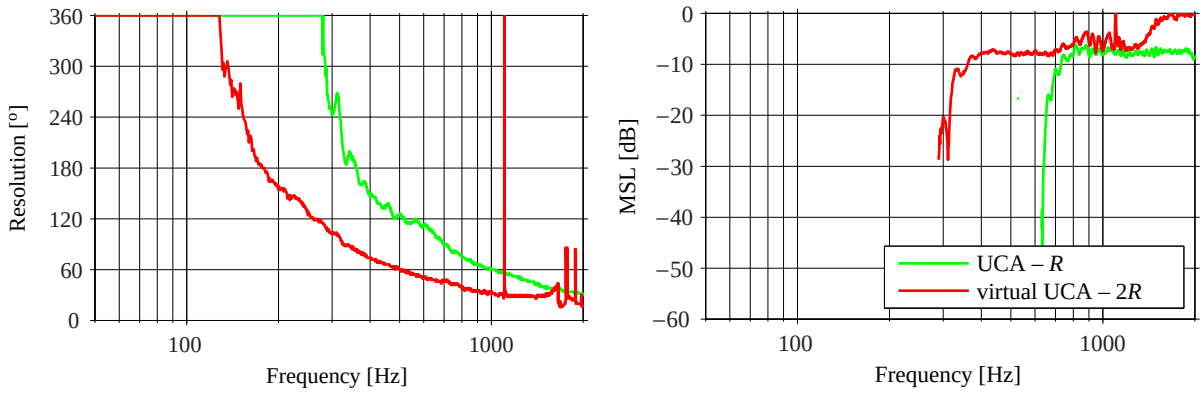

Fig. 8 – Resolution (left) and MSL (right) obtained with UCA of radius $R = 11.9$ cm and 12 microphones and a virtual UCA with radius $2R$. A plane wave was created by a source at $180°$.

acoustical holography. The predicted pressure is then used as input to the delay-and-sum beamforming algorithm. The benefits of using a virtual array have been proven by means of simulations and experimental results.

The combination of holography and beamforming adds new features to UCAs without any additional cost. Specifically the array gains more flexibility, for example at high frequencies the array measurements could be used directly for the beamforming procedure in the usual way, whereas at low frequencies acoustic holography could be used prior to beamforming to enhance the beamforming map at those frequencies.

There are still some questions that need to be examined further, e.g., the effect of using other beamforming techniques different from delay-and-sum beamforming, the applicability of the method in noisier conditions, and how large the virtual array can be. In this sense virtual arrays with radius larger than twice the radius of the actual array have been tested. The results, which are not included in the article, reveal that both resolution and MSL become worse than expected with increasing the radius. However this statement needs additional investigation.

The idea presented in the present study can be applied to other UCAs mounted on a scatterer such as a rigid cylinder, or to spherical arrays to map a three dimensional sound field.

ACKNOWLEDGMENTS

The authors are thankful to Finn Jacobsen who was involved in this study at an early stage.

REFERENCES

[1] E. Tiana-Roig, F. Jacobsen, and E. Fernandez-Grande, “Beamforming with a circular microphone array for localization of environmental noise sources”, J. Acoust. Soc. Am. **128(6)**, 3535–3542 (2010).

[2] G. Daigle, M. Stinson, and J. Ryan, “Beamforming with air-coupled surface waves around a sphere and circular cylinder (L)”, J. Acoust. Soc. Am. **117(6)**, 3373–3376 (2005).

[3] H. Teutsch and W. Kellermann, “Acoustic source detection and localization based on wavefield decomposition using circular microphone arrays”, J. Acoust. Soc. Am. **120(5)**, 2724–2736 (2006).

[4] E. Tiana-Roig, F. Jacobsen, and E. Fernandez-Grande, “Beamforming with a circular array of microphones mounted on a rigid sphere (L)”, J. Acoust. Soc. Am. **130(3)**, 1095–1098 (2011).

[5] E. Tiana-Roig and F. Jacobsen, “Acoustical source mapping based on deconvolution approaches for circular microphone arrays”, in *Proceedings of Inter-noise 2011, Osaka, Japan* (2011).

[6] E. Tiana-Roig and F. Jacobsen, “Deconvolution for the localization of d sources using a circular microphone array,”, J. Acoust. Soc. Am. (To be published).

[7] E. G. Williams, *Fourier Acoustics: Sound radiation and near field acoustic holography* (Academic, London) (1999).

[8] J. D. Maynard, E. G. Williams, and Y. Lee, “Nearfield acoustic holography : I . Theory of generalized holography and the development of NAH”, J. Acoust. Soc. Am. **78(4)**, 1395–1413 (1985).

[9] E. G. Williams, N. Valdivia, and P. C. Herdic, "Volumetric acoustic vector intensity imager", J. Acoust. Soc. Am. **120(4)**, 1887–1897 (2006).

[10] E. G. Williams and K. Takashima, "Vector intensity reconstructions in a volume surrounding a rigid spherical microphone array", J. Acoust. Soc. Am. **127(2)**, 773–783 (2010).

[11] F. Jacobsen, G. M. Pescador, E. Fernandez-Grande, and J. Hald, "Near field acoustic holography with microphones on a rigid sphere (L)", J. Acoust. Soc. Am. **129(6)**, 3461–3464 (2011).

[12] A. Granados, F. Jacobsen, and E. Fernandez-Grande, "Regularized reconstruction of sound fields with a spherical microphone array", in *ICA 2013 Montreal, Montreal, Canada* (2013).

[13] D. Johnson and D. Dudgeon, *Array Signal Processing Concepts and Techniques* (Prentice Hall, Englewood Cliffs, New Jersey) (1993).

[14] J. Meyer, "Beamforming for a circular microphone array mounted on spherically shaped objects", J. Acoust. Soc. Am. **109(1)**, 185–193 (2001).